# Observation of the Mollow Triplet from an optically confined single atom

Boon Long Ng,[1] Chang Hoong Chow,[1] and Christian Kurtsiefer[1, 2]

[1] *Center for Quantum Technologies, 3 Science Drive 2, Singapore 117543*
[2] *Department of Physics, National University of Singapore, 2 Science Drive 3, Singapore 117542**

(Dated: November 16, 2022)

Resonance fluorescence from atomic systems consists of a single spectral peak that evolves into a Mollow triplet for a strong excitation field. Photons from different peaks of the triplet show distinct ~~photon correlation~~ timing correlations that make the fluorescence a useful light source for quantum information ~~purpose~~purposes. We characterize the fluorescence of a single optically trapped $^{87}$Rb atom that is excited resonantly at different power levels. Second-order correlation measurements reveal the single photon nature of the fluorescence concurrently with Rabi oscillations of a strongly excited atom. The asymmetry in correlations between photons from two sidebands of the fluorescence spectrum when the atom is exposed to an off-resonant field ~~further~~ indicates that there is a preferred time-ordering of the emitted photons from different sidebands[1–5].

## I. INTRODUCTION

The investigation of fluorescence emitted from resonantly excited atomic systems has played a major role in understanding the interaction between atom and radiation [6]. In 1930, Weisskopf first established the theory of atomic resonance fluorescence in the limit of weak excitation [7]. In this limit, the fluorescence spectrum of a two-level atom shows a single scattering peak centered at the excitation frequency. The single peak consists mostly of coherent scattering and had been measured in various systems [8–10], which is a promising way to generate highly coherent single photons with subnatural linewidth [11, 12].

Later this result was extended to include the effect of strong excitation radiation by Mollow in 1969 [13]. When the driving intensity increases above the saturation regime, the ~~inelastic~~ incoherent component in the fluorescence dominates, and the single peak spectrum evolves into a triplet structure. The photons emitted in this process continue to be of interest in quantum optics, as these photons exhibit different correlation signatures in particular conditions such as off-resonant excitation [1–5, 14, 15]. There has been renewed interest in photon statistics of the coherent and incoherent component that coexist in the fluorescence. With better filtering techniques that are available nowadays, the photon correlation from these two components can be measured independently [16–18].

The Mollow triplet was first observed experimentally in an atomic beam passing perpendicularly through an intense laser field [19–21] where the emitted fluorescence spectrum was analyzed using a Fabry-Perot cavity. This configuration minimized Doppler broadening due to atomic motion ~~,~~and the fluorescence could be approximated as light emitted from individual non-interacting atoms. Since then, the Mollow triplet has been successfully observed in many different systems such as quantum dots ~~[3, 10, 23–25]~~[3, 10, 22–25], molecules [26], ions [27, 28], cold atomic cloud [29], and superconducting qubits [30–32].

While easier to implement experimentally, light interaction with an ensemble of atoms will mask certain features of the process such as photon anti-bunching. In contrast, a single optically trapped atom is an excellent candidate to investigate photon correlations between different frequency components in the Mollow triplet. An optically confined atom can be cooled to sub-Doppler temperature owing to polarization gradient cooling (PGC) [33, 34], and therefore suppresses the Doppler contribution to the spectrum. Using a magnetic field to lift the Zeeman degeneracy and an appropriate driving laser polarization, the closed transition of an ideal two-level system can be implemented, coming close to the ideal situation considered in the Mollow triplet theory.

In this paper, we report the observation and analysis of fluorescence collected from a strongly driven single $^{87}$Rb atom in a far off-resonance optical dipole trap (FORT). An aspherical lens focuses near-resonant probe laser light onto the atom and collects backscattered photons with minimal laser background. The probe is near-resonant with the closed transition $5S_{1/2}\,|F=2,\ m_F=-2\rangle \equiv |g\rangle$ to $5P_{3/2}\,|F=3,\ m_F=-3\rangle \equiv |e\rangle$. We analyze the spectrum of the light scattered by the atom at different excitation intensities with a scanning Fabry-Perot cavity. A second-order photon correlation measurement of the fluorescence shows the signature Rabi oscillation with frequency that relates to the driving intensity. Under off-resonant excitation, the temporal cross-correlation between photons originating from different sidebands is measured to reveal the dynamics of the underlying optical transitions. The preferred time-ordering of the emitted photons from opposite sidebands could prove to be useful as a heralded narrowband single photon source, or a quantum resource in quantum network where quantum information is stored and processed at a stationary node, which could be atomic ensemble [35] or a single atom within a cavity [36, 37].

* christian.kurtsiefer@gmail.com

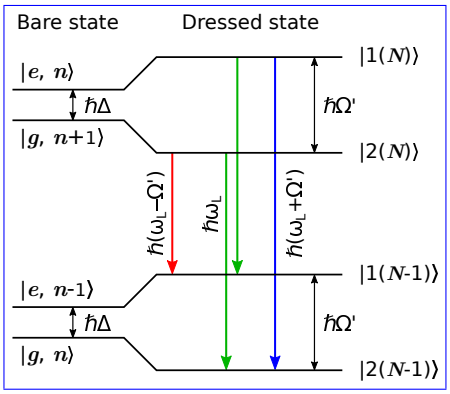


FIG. 1. Dressed-state picture for an atom coupling to an intense driving field. Bare states are characterized by the photon number Fock state ($n$), and the atom in the ground ($g$) or excited ($e$) state. Their energy difference is $\hbar\Delta$ in the rotating frame, where $\Delta$ is detuning of the driving field from atomic resonance. Dressed states are described by a pair of states with a number of total excitations, $N$, split by $\hbar\Omega'$ with a generalized Rabi frequency $\Omega' = \sqrt{\Omega^2 + \Delta^2}$.

## II. THEORETICAL BACKGROUND

~~In the limit~~ Assuming a weak monochromatic driving field, the light will be scattered elastically by the atom. The coherent component of the atomic fluorescence that consists of this elastically scattered light shows a sharp peak at the driving frequency in the spectrum that resembles that of the driving field. As the driving intensity increases, incoherently scattered light starts to appear in the spectrum, while the coherent component will gradually reduce. The incoherent component dominates the spectrum as Rabi frequency $\Omega$ increases and the sidebands begin to emerge.

In the regime of a strong driving field ~~($\Omega \gg \Gamma/4$)~~($\Omega > \Gamma/4$), the power spectrum of the resonance fluorescence ~~is given by~~ can be decomposed into a coherent component, $S_{\rm coh}(\omega)$, and an incoherent component, $S_{\rm incoh}(\omega)$:

$$S(\omega) = S_{\rm coh}(\omega) + S_{\rm incoh}(\omega), \tag{1}$$

with

$$S_{\rm coh}(\omega) = \frac{s}{(1+s)^2}\delta(\omega), \tag{2}$$

$$\begin{aligned} S_{\rm incoh}(\omega) = {} & \frac{s}{8\pi(1+s)}\frac{\Gamma}{\omega^2 + (\Gamma/2)^2} \\ & + \frac{s}{32\pi(1+s)^2}\frac{3\Gamma(s-1) + \frac{\Gamma}{\Omega}(5s-1)(\omega+\Omega)}{(\omega+\Omega)^2 + (3\Gamma/4)^2} \\ & + \frac{s}{32\pi(1+s)^2}\frac{3\Gamma(s-1) - \frac{\Gamma}{\Omega}(5s-1)(\omega-\Omega)}{(\omega-\Omega)^2 + (3\Gamma/4)^2}, \end{aligned} \tag{3}$$

where $\omega$ is the relative frequency from the monochromatic driving field ~~, $\Omega$ is the Rabi frequency~~ and $\Gamma$ represents the natural linewidth of the atomic transition, which in this case is $2\pi \times 6.07\,\mathrm{MHz}$ for $^{87}$Rb D2 transition. The resonant saturation parameter $s = 2\Omega^2/\Gamma^2$ characterizes how strongly the atom is driven, and determines the strength of coherent and incoherent components in the fluorescence.

~~According to Eqn~~The coherent component is characterized by a Dirac delta function at the driving frequency (Eq. ~~(1), the power spectrum contains a 2))~~, while $S_{\rm incoh}(\omega)$ has a central resonant Lorentzian peak with a full width half maximum (FWHM) of $\Gamma$ ~~and~~ as well as two side peaks ~~located at~~ $\pm\Omega$ away from the resonance, with a FWHM of $3\Gamma/2$. These sidebands, together with the central peak, form the Mollow triplet. The coherent component dominates the spectrum over the incoherent one when $s$ is small, reaches an absolute maximum at $s = 1$, and decreases when $s$ gets larger while the incoherent contribution saturates. This result was derived by Mollow using a semi-classical approach [13], but the same result can be obtained using a fully quantum-mechanical picture [38].

One way to interpret the spectral features is to describe the atomic energy states as dressed by the driving field [15, 39]. In ~~this~~ the dressed-state picture, the new eigenstates are a superposition of the bare states $|g, n+1\rangle$ and $|e, n\rangle$, where "~~g~~$g$" and "~~e~~$e$" refer to the ground and excited states of the atom, while $n$ indicates the number of photons from the driving field (see Fig. 1). In every manifold where the total number ~~$N$ of photons plus atomic excitation~~ of excitations, $N$, is the same, the eigenstates are split by the Rabi frequency for on-resonance excitation.

The three frequency components in the fluorescence can be explained by spontaneous decay from a manifold of $N$ total excitations to a manifold with $(N-1)$ excitations. Four optical transitions are possible in this process. Two of them are degenerate (green decays in Fig. 1) and correspond to the central peak in the fluorescence spectrum, while the sidebands $\pm\Omega$ away from the central peak originate from the other two transitions (red and blue decays in Fig. 1). This leads to the ~~weightage~~ weighting of 1:2:1 in the total spectral intensities of the incoherent peaks under resonant excitation. Note that this picture is most useful when $\Omega \gg \Gamma$ where the dressed states are spectrally resolved.

## III. EXPERIMENTAL SETUP

Our experiment starts with a single $^{87}$Rb atom trapped in a red-detuned FORT that is loaded from a magneto-optical trap (MOT) (see Fig. 2). This dipole trap is formed by a linearly polarized Gaussian laser beam (wavelength 851 nm) that is tightly focused by a pair of high numerical aperture lenses (NA = 0.75, focal length $f = 5.95\,\mathrm{mm}$) to a waist of $w_0 = 1.1\,\mu\mathrm{m}$. Part of the

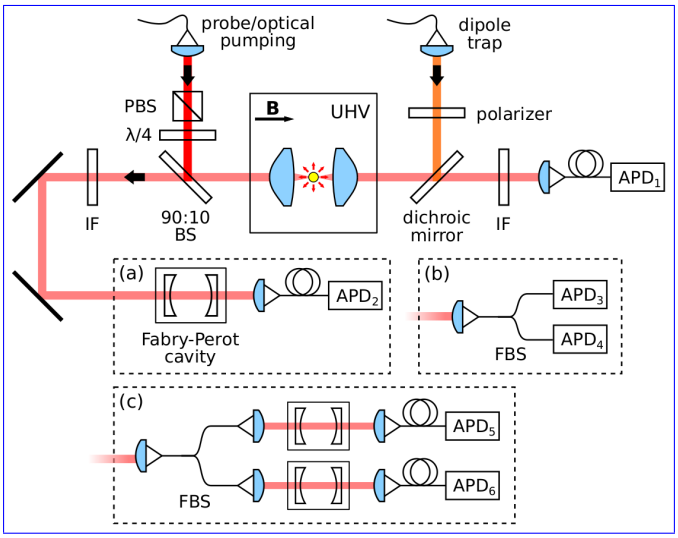


FIG. 2. Setup for probing light-atom interaction in free space. A single $^{87}$Rb atom is cooled and trapped in a far off-resonance dipole trap. One avalanche photodetector ($APD_1$) is used to monitor the atomic fluorescence ~~which act~~ and acts as a trigger to start ~~experiment~~ the experimental sequence. (a) A Fabry-Perot cavity is placed before ~~another~~ $APD_2$ to ~~measure~~ record the frequency spectrum of the atomic fluorescence. (b) ~~Hanbury Brown~~ Hanbury-Brown and Twiss (HBT) configuration to measure second-order intensity autocorrelation. (c) Cross-correlation measurement setup ~~by placing~~ with a cavity in each arm before ~~each~~ $APD_5$ and $APD_6$ to select ~~photon~~ photons from specific frequency ~~window~~windows. UHV: ultra-high vacuum chamber, IF: interference filter centered at 780 nm, $\lambda/4$: quarter-wave plate, PBS: polarizing beam splitter, FBS: fiber beam splitter, B: magnetic field.

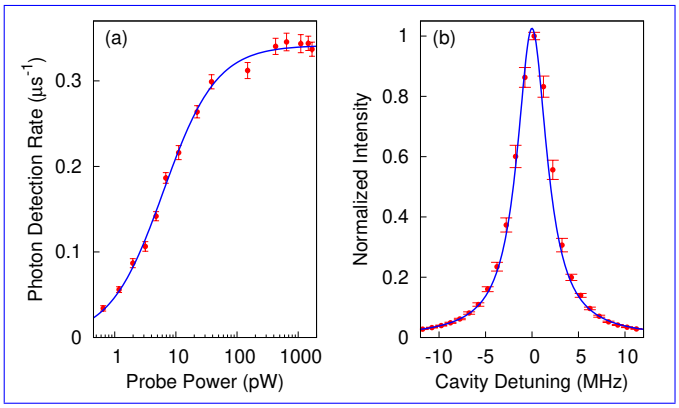


FIG. 3. (a) Resonant saturation measurement, with the blue solid line representing the fit to $\frac{\eta\Gamma}{2}\frac{P_{\rm probe}}{P_{\rm probe}+P_{\rm sat}}$ with saturation power $P_{\rm sat} = 6.3(2)$ pW and total detection efficiency $\eta = 1.79(2)\,\%$. Here, $P_{\rm probe}$ is incident probe power. (b) Cavity transmission of the probe laser to characterize the cavity linewidth.

atomic fluorescence is collected through the same lenses and coupled into single mode fibers that are connected to avalanche photodetectors (APD).

Once an atom is trapped, we apply 10 ms of PGC to reduce the atomic motion to a temperature of 14.7(2) $\mu$K [40], corresponding to a Doppler broadening of 113 kHz. Then, a bias magnetic field of 1.44 mT is applied along the FORT laser propagation direction to remove the degeneracy of the Zeeman states, and the atom is optically pumped into $|g\rangle$ [41]. Next, we turn on the probe laser beam along the optical axis for 2 $\mu$s. This pulse length is chosen to maximize the duty cycle of photon collection while avoiding excessive recoil heating of the atom. The probe frequency is locked to the $F = 2 \rightarrow F' = 3$ hyperfine transition of the $^{87}$Rb $D_2$ line, and shifted by an acousto-optic modulator (AOM) in order to address the $|g\rangle \leftrightarrow |e\rangle$ transition. The probe is prepared into a $\sigma^-$ polarization with a quarter-wave plate after a polarizing beam splitter (PBS) to target the closed transition.

We collect photons scattered backwards through the same lens and couple them into a single mode fiber, avoiding the strong light levels of the probe laser for analysis. The photon scattering rate is first characterized for different intensity levels of the probe field, as illustrated in Fig. 3(a). The atomic response saturates at a probe power of 6.3(2) pW and total detection efficiency, $\eta = 1.79(2)\,\%$ can be inferred from the fit.

The collected photons are frequency-filtered with a Fabry-Perot cavity and subsequently detected with ~~an APD~~$APD_2$. By scanning the cavity resonance frequency, the frequency spectrum of the fluorescence can be obtained. To precisely control the resonance frequency of this cavity, it is locked to a tunable sideband generated by an electro-optical modulator (EOM) from another laser locked to the D1 transition of $^{87}$Rb. The linewidth of the cavity is characterized to be 3.92(5) MHz with an external cavity diode laser (see Fig. 3(b)). This value will be used for deconvolution of the atomic spectrum in the next part of this paper.

Figure 4 shows a series of frequency spectra for increasing excitation powers. At weak excitation, the FWHM of the single peak in Fig. 4(a) is 2.5(3) MHz after deconvolution from the cavity contribution. This shows that at a driving power that is well below saturation, the coherent component with linewidth smaller than $\Gamma$ dominates the spectrum.

As the power increases, the three-peak structure emerges and the splitting between the peaks also increases. The fit to the experimental data is done with ~~Eqn~~Eq. (1) convoluted with the cavity transfer function. After excluding cavity contribution, the central peak in Fig. 4(e) has a FWHM of ~~7.3(5~~7.8(3) MHz extracted from the fit. This value is close to the atomic natural linewidth of $^{87}$Rb, thus justifying the claim that an optically trapped single atom can be laser cooled to mitigate the Doppler broadening effect.

Theoretically, the height ratio between the central peak and the sidebands is 1 : 3 : 1 according to ~~Eqn~~Eq. (1), owing to the fact that the sidebands have a larger width

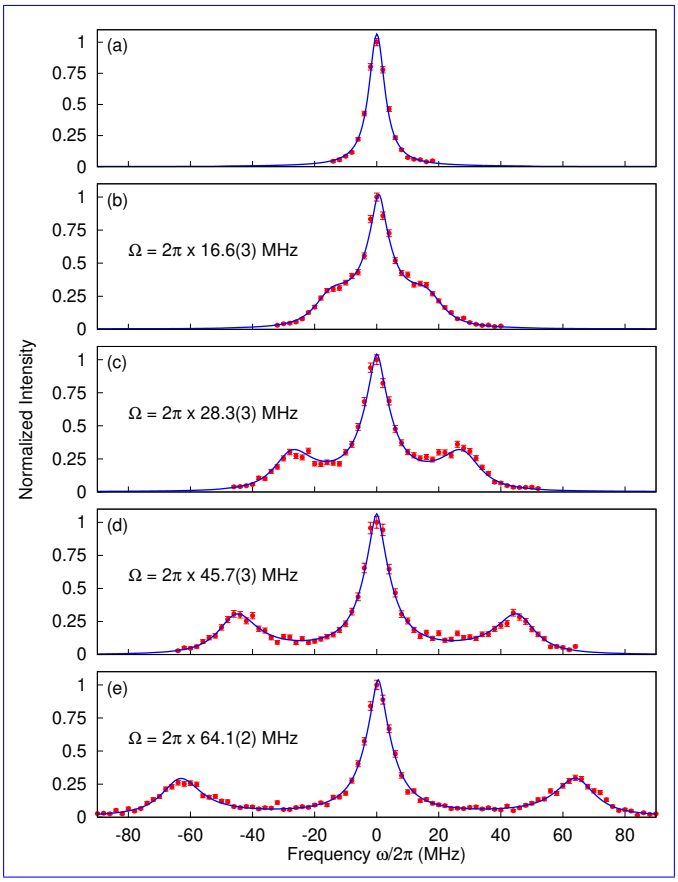


FIG. 4. Normalized resonance atomic emission spectra at different excitation intensities recorded by scanning the Fabry-Perot cavity with the setup in Fig. 2(a). For (b)-(e), the solid line is a fit to Eq. (1) convoluted with the cavity transfer function and the effect of laser reflection. The Rabi frequency Ω extracted from the fit is labeled in Fig. 4(b)-(e).

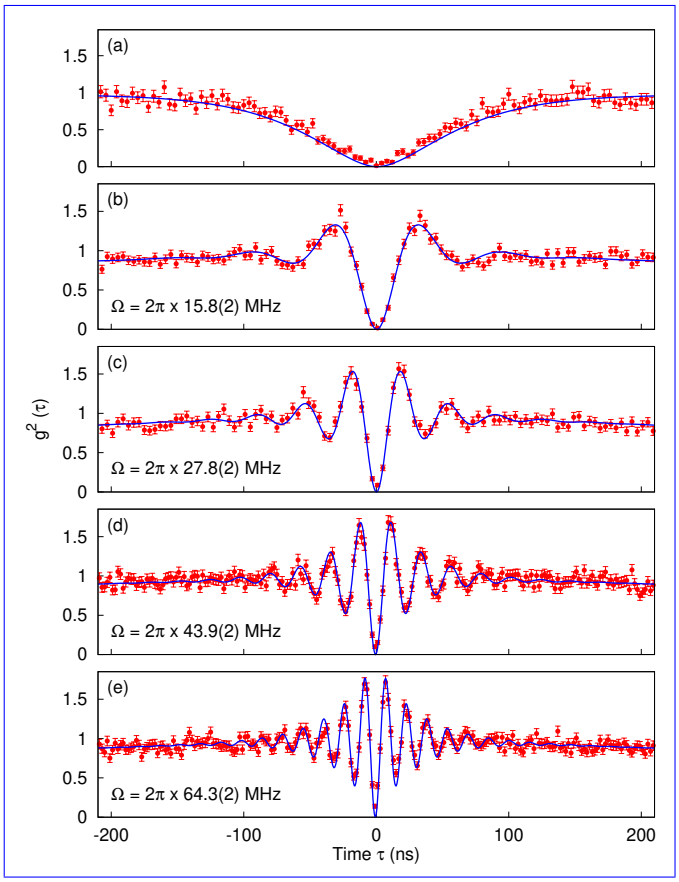


FIG. 5. Second-order correlation function of the single atom at different excitation intensities. The solid line is a fit to Eq. (4) with ~~addition~~ inclusion of triangle function ~~resulted~~ resulting from a convolution of two square pulses. The Rabi frequency Ω ~~extracted from the fit is labeled in Fig. 5(b)-(e)~~ shown for each spectrum is extracted from the respective fit.

compared to the central peak. After taking into account the cavity contribution, the height of the central peak should decrease such that the ratio reaches around 1 : 2.6 : 1. However, the measured spectra show central peaks with about 3.7 times the height of sidebands (average value of Fig. 4(c)-(e)). This inconsistency between the theoretical prediction and the experimental data can be likely attributed to the reflection and scattering of the probe laser from the optics. Taking this reflection into consideration by adding a term to Eq. (1) that scales with power in a model to describe our experiment, we can extract how much power from the observed spectrum can be attributed to such a reflection. We characterized this laser reflection from the fit and found a contribution of ~~around 7.6~~0.9 %, 2.4 % and 4.5 % of the total power in the ~~spectrum.With addition of this contribution, the calculation shows that the ratio after cavity convolution will be 1 : 3.7 : 1 , which explain the measurement results.~~ spectra (c)-(e) in Fig. 4.

## IV. SECOND ORDER CORRELATION FUNCTION

In the subsequent part of the experiment, we replace the Fabry-Perot cavity with a fiber beam splitter and two APDs in a Hanbury-Brown and Twiss configuration as shown in Fig. 2(b) [42]. The arrival time of the photons is recorded. The second-order intensity correlation function ($g^{(2)}(\tau)$) of the atomic fluorescence can be inferred from this measurement. This correlation function can reveal some characteristics of the photons emitted by single atom such as photon anti-bunching. It was first demonstrated experimentally by Kimble *et al.* in 1977 [43] which showed that fluorescence from a two-level atom is manifestly quantum. While a vanishing second-order intensity correlation of the fluorescence at zero delay is a clear indication for this phenomenon, the dynamic of $g^{(2)}(\tau)$ near the zero delay reveals more about the underlying atom-light interaction such as a Rabi oscillation.

For driving fields of low intensity, $g^{(2)}(\tau)$ shows a monotonic increase to unity as $\tau$ increases from zero to

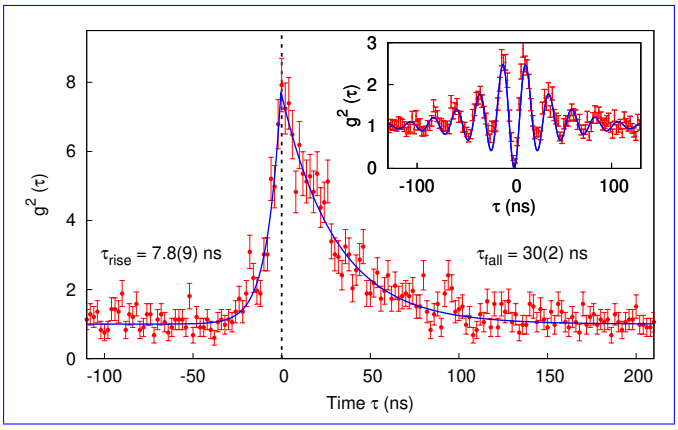


FIG. 6. Normalized cross-correlation between photons from two opposite Mollow sidebands as a function of delay $\tau$ between detection of a photon from the higher energy sideband after detection of a photon from lower energy sideband. Inset: Normalized intensity autocorrelation of the unfiltered off-resonance atomic fluorescence to extract $\Omega'$.

much larger than $1/\Gamma$. When the driving field intensity increases above ~~the~~ saturation, $g^{(2)}(\tau)$ resembles the case for weak excitations at large delay, but oscillations corresponding to the Rabi frequency appear around zero delay. Upon ~~the detection of~~ detection of the first fluorescence photon, the atom is being projected onto the ground state and the probability to detect the subsequent photon at some later time, $\tau$ is proportional to the excited state population of the atom. This correlation function for fluorescence from a single atom can be expressed as [44]

$$g^{(2)}(\tau) = 1 - e^{-(3\Gamma/4)|\tau|}\left(\cos\Omega\tau + \frac{3\Gamma}{4\Omega}\sin\Omega|\tau|\right). \quad (4)$$

The correlation measurements shown in Fig. 5 are fitted using ~~Eqn~~Eq. (4), multiplied with a triangle function that results from convolution of two square pulses of the same length. This is done to account for fluorescence from each detector being collected during a $2\,\mu$s wide time window. The correlation between two such windows will result in a $4\,\mu$s wide triangular envelope. The Rabi frequency $\Omega$ can be also extracted from the fit, and it serves as an independent measurement allowing comparison to the values obtained from the Mollow triplet measurement. The extracted values, shown in Fig. 5 for different driving powers, agree well with the values for $\Omega$ obtained from the Mollow triplet spectra.

## V. OFF-RESONANT EXCITATION

While the atom is excited resonantly, the emission of the sideband photons does not have a preferred order. As such, the cross-correlation between photons from different sidebands is symmetric with respect to zero time delay, $\tau = 0$. However, if the excitation field is detuned from the atomic resonance, this symmetry is broken as the emission process of the sideband photons now have a preferred order [1–3, 15]. The preferred order of the emission depends on the sign of the detuning and manifests as an asymmetry in the correlation measurement around $\tau = 0$.

In this part of the experiment, we red-detune the excitation laser by 30 MHz from the atomic resonance. As shown in Fig. 2(c), there is a Fabry-Perot cavity in front of each APD to filter the incoming fluorescence such that photon correlation between chosen spectral components can be measured. To better transmit the photons from different peaks, the cavities used in this experiment have linewidth of 20 MHz.

The spectrum of the fluorescence is slightly different when the atom is excited off-resonantly, with the central peak sitting at the driving frequency, and the sideband are separated from the central peak by the generalized Rabi frequency, $\Omega' = \sqrt{\Omega^2 + \Delta^2}$, where $\Delta$ is the detuning of the laser from atomic resonance. The power ratio between the central peak and the sidebands deviates from the on-resonance case, with the central peak being suppressed as detuning increases. In order to align the cavity resonance with the respective sidebands, we first measure the second-order correlation of the off-resonance fluorescence. The data is shown in the inset of Fig. 6 and the blue solid line is the fit to extract $\Omega'$, which is $2\pi \times 42(1)$ MHz in this case. As such, the cavity resonance is locked at $\pm\Omega'$ away from the driving frequency to isolate the sidebands photon.

Figure 6 shows the cross-correlation measurement between the opposite Mollow sidebands where we use photon from the lower energy sideband as 'start' trigger and the photon from the other sideband as 'stop' signal. The measurement shows a clear bunching behavior around $\tau = 0$. We normalize the correlation function with respect to coincidence counts from a time window that is far from $\tau = 0$. With this, we obtain a bunching value of 8.1(8). The normalized correlation is then fitted by two exponentials, with time constants of $\tau_{\rm rise} = 7.8(9)$ ns and $\tau_{\rm fall} = 30(2)$ ns, respectively. The theoretical prediction following [2] for $\tau_{\rm rise}$ and $\tau_{\rm fall}$ are 7.96 ns and 35.02 ns, respectively. The asymmetry of the correlation function ~~justifies the claim~~ indicates that the emission of the ~~sidebands photon~~ sideband photons has a preferred time-order for off-resonant excitation, ~~which~~ in this case ~~photon~~ first an emission from the lower energy sideband~~followed by photon~~, followed by a second emission from the higher energy sideband~~forms a temporal cascade emission~~.

Using Eq. (40) from [2], the theoretically predicted bunching value is 11 for the parameters in our experiment. The discrepancy to our observed value of 8.1 can be attributed to the imperfection in spectral filtering process. With separation of 42(1) MHz, cavities with a linewidth of 20 MHz cannot suppress the photons from the central peak and the opposite sideband entirely. Therefore, there are some correlation contributions from different combinations of photons in our experiment, for

example between photons from the central peak and photons from two sidebands. These would reduce the expected bunching value.

## VI. CONCLUSION

In summary, we have measured the frequency spectrum of the resonance fluorescence of an optically trapped atom at different excitation intensities, until the emitter is saturated. The distinctive Mollow triplet has been observed and has been compared to the theoretical model. After taking into account the effect of the cavity transfer function and excitation power fluctuations, our results agree with the theoretical prediction very well. For each excitation intensity used in the measurements of the emission spectra, we also record the second order correlation function of the atomic fluorescence. The Rabi frequency can be extracted by fitting $g^{(2)}(\tau)$ and this value serves as a benchmark for the results obtained in each measured spectrum. With off-resonant excitation, the photons from opposite sidebands have a preferred order of emission which is reflected in the asymmetry of the correlation around $\tau = 0$. ~~This can be useful when using a single atom as~~ Such a preferred time-ordering of the emitted photons from opposite sidebands could be a used in a heralded narrowband single photon source ~~, or a quantum resource in quantum network where the quantum information is stored and processed through a node, which could be atomic ensemble [35] or a single atom within a cavity [36, 37]~~ that might find applications in quantum networks using atoms or atom-like systems as stationary nodes.

## ACKNOWLEDGMENTS

We acknowledge support of this work by the Ministry of Education in Singapore and the National Research Foundation, Prime Minister's office, through the Research Centres of Excellence programme.

## Appendix A SINGLE ATOM TRAPPING

We first form a cloud of $^{87}$Rb atoms using a magneto-optical trap (MOT) inside an ultra-high vacuum chamber (UHV). In order to load a single atom, the MOT is spatially overlapped with the optical dipole trap. This dipole trap is formed by a linearly polarized Gaussian laser beam (wavelength 851 nm) that is tightly focused by a pair of high numerical aperture lenses (NA = 0.75, focal length $f = 5.95$ mm) to a waist of $w_0 = 1.1\,\mu$m.

We collect the fluorescence from the atom through the same lens and couple it into a single mode optical fiber connected to avalanche photodetector $APD_1$. When a single atom enters the dipole trap, the count rate at $APD_1$ increases from $200\,s^{-1}$ to $7000\,s^{-1}$. Our experimental control system collects this fluorescence during a qualifying time window of 20 ms. If more than 40 photoevents are detected in this window (corresponding to a rate of $2000\,s^{-1}$), an atom was loaded into the dipole trap with a high probability; otherwise, the next qualifying window is started. On qualification, the system branches to a sequence where the MOT is turned off to prevent collisional losses, and the spectroscopy on the single atom is carried out. Lastly, a second qualifying test with the MOT turned on allows to exclude measurements where the atom was lost, and to laser-cool the atom to remove momentum gained by the scattering experiment. The conditional experimental sequencing technique is similar to [45].

## Appendix B NARROW-BAND SPECTRAL FILTERING

The cavities used in these experiments are simple Fabry-Perot resonators formed by two mirrors, with a piezo actuator to tune the cavity resonance. The cavity resonance is locked to a light from the 795 nm repump laser for the MOT operation that itself is locked to the $|5S_{1/2}, F = 1\rangle \rightarrow |5P_{1/2}, F = 2\rangle$ transition of $^{87}$Rb in a gas cell. Light at 795 nm can be easily separated from the fluorescence light (780 nm) with an interference filter so that it will not affect the fluorescence measurements a the single photon level.

The tunability of the filter cavity frequency is accomplished by using a sideband of the original 795 nm pumping light for the lock, generated by an electro-optical modulator (EOM) driven by a tuneable radio frequency signal.

[1] A. Aspect, G. Roger, S. Reynaud, J. Dalibard, and C. Cohen-Tannoudji, Time correlations between the two sidebands of the resonance fluorescence triplet, Phys. Rev. Lett. **45**, 617 (1980).
[2] C. A. Schrama, G. Nienhuis, H. A. Dijkerman, C. Steijsiger, and H. G. M. Heideman, Intensity correlations between the components of the resonance fluorescence triplet, Phys. Rev. A **45**, 8045 (1992).
[3] A. Ulhaq, S. Weiler, S. M. Ulrich, R. Roßbach, M. Jetter, and P. Michler, Cascaded single-photon emission from the Mollow triplet sidebands of a quantum dot, Nature Photonics **6**, 238 (2012).
[4] M. Peiris, B. Petrak, K. Konthasinghe, Y. Yu, Z. C. Niu, and A. Muller, Two-color photon correlations of the light

scattered by a quantum dot, Phys. Rev. B **91**, 195125 (2015).
[5] J. C. López Carreño, E. del Valle, and F. P. Laussy, Photon correlations from the Mollow triplet, Laser and Photonics Reviews **11**, 1700090 (2017).
[6] H. Walther, Resonance fluorescence of two-level atoms, in *Advances In Atomic, Molecular, and Optical Physics*, Vol. 51 (Academic Press, 2005) pp. 239–272.
[7] V. Weisskopf and E. Wigner, Berechnung der natürlichen linienbreite auf grund der diracschen lichttheorie, Zeitschrift für Physik **63**, 54 (1930).
[8] H. Gibbs and T. Venkatesan, Direct observation of fluorescence narrower than the natural linewidth, Optics Communications **17**, 87 (1976).
[9] J. T. Höffges, H. W. Baldauf, W. Lange, and H. Walther, Heterodyne measurement of the resonance fluorescence of a single ion, Journal of Modern Optics **44**, 1999 (1997).
[10] K. Konthasinghe, J. Walker, M. Peiris, C. K. Shih, Y. Yu, M. F. Li, J. F. He, L. J. Wang, H. Q. Ni, Z. C. Niu, and A. Muller, Coherent versus incoherent light scattering from a quantum dot, Phys. Rev. B **85**, 235315 (2012).
[11] H. S. Nguyen, G. Sallen, C. Voisin, P. Roussignol, C. Diederichs, and G. Cassabois, Ultra-coherent single photon source, Applied Physics Letters **99**, 261904 (2011).
[12] C. Matthiesen, A. N. Vamivakas, and M. Atatüre, Subnatural linewidth single photons from a quantum dot, Phys. Rev. Lett. **108**, 093602 (2012).
[13] B. R. Mollow, Power spectrum of light scattered by two-level systems, Phys. Rev. **188**, 1969 (1969).
[14] C. Cohen-Tannoudji and S. Reynaud, Atoms in strong light-fields: photon antibunching in single atom fluorescence, Philosophical Transactions of the Royal Society of London. Series A, Mathematical and Physical Sciences **293**, 223 (1979).
[15] G. Nienhuis, Spectral correlations in resonance fluorescence, Phys. Rev. A **47**, 510 (1993).
[16] L. Hanschke, L. Schweickert, J. C. L. Carreño, E. Schöll, K. D. Zeuner, T. Lettner, E. Z. Casalengua, M. Reindl, S. F. C. da Silva, R. Trotta, J. J. Finley, A. Rastelli, E. del Valle, F. P. Laussy, V. Zwiller, K. Müller, and K. D. Jöns, Origin of antibunching in resonance fluorescence, Phys. Rev. Lett. 125, 170402 (2020).
[17] C. L. Phillips, A. J. Brash, D. P. S. McCutcheon, J. Iles-Smith, E. Clarke, B. Royall, M. S. Skolnick, A. M. Fox, and A. Nazir, Photon statistics of filtered resonance fluorescence, Phys. Rev. Lett. 125, 043603 (2020).
[18] L. Masters, X. Hu, M. Cordier, G. Maron, L. Pache, A. Rauschenbeutel, M. Schemmer, and J. Volz, Will a single two-level atom simultaneously scatter two photons? (2022), arXiv:2209.02547 [quant-ph].
[19] F. Schuda, C. R. Stroud, and M. Hercher, Observation of the resonant stark effect at optical frequencies, Journal of Physics B: Atomic and Molecular Physics **7**, L198 (1974).
[20] W. Hartig, W. Rasmussen, R. Schieder, and H. Walther, Study of the frequency distribution of the fluorescent light induced by monochromatic radiation, Zeitschrift für Physik A Atoms and Nuclei **278**, 205 (1976).
[21] R. E. Grove, F. Y. Wu, and S. Ezekiel, Measurement of the spectrum of resonance fluorescence from a two-level atom in an intense monochromatic field, Phys. Rev. A **15**, 227 (1977).
[22] A. Muller, E. B. Flagg, P. Bianucci, X. Y. Wang, D. G. Deppe, W. Ma, J. Zhang, G. J. Salamo, M. Xiao, and C. K. Shih, Resonance fluorescence from a coherently driven semiconductor quantum dot in a cavity, Phys. Rev. Lett. 99, 187402 (2007).
[23] A. Nick Vamivakas, Y. Zhao, C.-Y. Lu, and M. Atatüre, Spin-resolved quantum-dot resonance fluorescence, Nature Physics **5**, 198 (2009).
[24] E. B. Flagg, A. Muller, J. W. Robertson, S. Founta, D. G. Deppe, M. Xiao, W. Ma, G. J. Salamo, and C. K. Shih, Resonantly driven coherent oscillations in a solid-state quantum emitter, Nature Physics **5**, 203 (2009).
[25] S. Ates, S. M. Ulrich, S. Reitzenstein, A. Löffler, A. Forchel, and P. Michler, Post-selected indistinguishable photons from the resonance fluorescence of a single quantum dot in a microcavity, Phys. Rev. Lett. **103**, 167402 (2009).
[26] G. Wrigge, I. Gerhardt, J. Hwang, G. Zumofen, and V. Sandoghdar, Efficient coupling of photons to a single molecule and the observation of its resonance fluorescence, Nature Physics **4**, 60 (2008).
[27] Y. Stalgies, I. Siemers, B. Appasamy, T. Altevogt, and P. E. Toschek, The spectrum of single-atom resonance fluorescence, Europhysics Letters (EPL) **35**, 259 (1996).
[28] J. D. Sterk, L. Luo, T. A. Manning, P. Maunz, and C. Monroe, Photon collection from a trapped ion-cavity system, Phys. Rev. A **85**, 062308 (2012).
[29] L. Ortiz-Gutiérrez, R. C. Teixeira, A. Eloy, D. F. da Silva, R. Kaiser, R. Bachelard, and M. Fouché, Mollow triplet in cold atoms, New Journal of Physics **21**, 093019 (2019).
[30] O. Astafiev, A. M. Zagoskin, A. A. Abdumalikov, Y. A. Pashkin, T. Yamamoto, K. Inomata, Y. Nakamura, and J. S. Tsai, Resonance fluorescence of a single artificial atom, Science **327**, 840 (2010).
[31] A. F. van Loo, A. Fedorov, K. Lalumire, B. C. Sanders, A. Blais, and A. Wallraff, Photon-mediated interactions between distant artificial atoms, Science **342**, 1494 (2013).
[32] D. M. Toyli, A. W. Eddins, S. Boutin, S. Puri, D. Hover, V. Bolkhovsky, W. D. Oliver, A. Blais, and I. Siddiqi, Resonance fluorescence from an artificial atom in squeezed vacuum, Phys. Rev. X **6**, 031004 (2016).
[33] P. J. Ungar, D. S. Weiss, E. Riis, and S. Chu, Optical molasses and multilevel atoms: theory, J. Opt. Soc. Am. B **6**, 2058 (1989).
[34] D. S. Weiss, E. Riis, Y. Shevy, P. J. Ungar, and S. Chu, Optical molasses and multilevel atoms: experiment, J. Opt. Soc. Am. B **6**, 2072 (1989).
[35] A. Kuzmich, W. P. Bowen, A. D. Boozer, A. Boca, C. W. Chou, L.-M. Duan, and H. J. Kimble, Generation of nonclassical photon pairs for scalable quantum communication with atomic ensembles, Nature **423**, 731 (2003).
[36] T. Wilk, S. C. Webster, A. Kuhn, and G. Rempe, Single-atom single-photon quantum interface, Science **317**, 488 (2007).
[37] S. Ritter, C. Nölleke, C. Hahn, A. Reiserer, A. Neuzner, M. Uphoff, M. Mücke, E. Figueroa, J. Bochmann, and G. Rempe, An elementary quantum network of single atoms in optical cavities, Nature **484**, 195 (2012).
[38] H. J. Kimble and L. Mandel, Theory of resonance fluorescence, Phys. Rev. A **13**, 2123 (1976).
[39] C. Cohen-Tannoudji and S. Reynaud, Dressed-atom description of resonance fluorescence and absorption spectra of a multi-level atom in an intense laser beam, Jour-

nal of Physics B: Atomic and Molecular Physics **10**, 345 (1977).
[40] Y.-S. Chin, M. Steiner, and C. Kurtsiefer, Polarization gradient cooling of single atoms in optical dipole traps, Phys. Rev. A **96**, 033406 (2017).
[41] C. H. Chow, B. L. Ng, and C. Kurtsiefer, Coherence of a dynamically decoupled single neutral atom, J. Opt. Soc. Am. B **38**, 621 (2021).
[42] R. H. Brown and R. Q. Twiss, Correlation between photons in two coherent beams of light, Nature **177**, 27 (1956).
[43] H. J. Kimble, M. Dagenais, and L. Mandel, Photon antibunching in resonance fluorescence, Phys. Rev. Lett. **39**, 691 (1977).
[44] R. Loudon, *The quantum theory of light* (OUP Oxford, 2000).
[45] M. Weber, J. Volz, K. Saucke, C. Kurtsiefer, and H. Weinfurter, Analysis of a single-atom dipole trap, Phys. Rev. A **73**, 043406 (2006)
.